journal of materials processing technology 202 (2008) 22–26

journal homepage: www.elsevier.com/locate/jmatprotec

Active soldering of $ZnS–SiO_2$ sputtering targets to copper backing plates using an Sn3.5Ag4Ti(Ce, Ga) filler metal

S.Y. Chang[a,*], T.H. Chuang[b], L.C. Tsao[b], C.L. Yang[a], Z.S. Yang[a]

[a] Department of Mechanical Engineering, National Yunlin University of Science & Technology, 640 Touliu, Taiwan
[b] Department of Materials Science and Engineering, National Taiwan University, 106 Taipei, Taiwan

ARTICLE INFO

Article history:
Received 7 February 2007
Received in revised form
11 June 2007
Accepted 30 August 2007

Keywords:
Active soldering
$ZnS–SiO_2$
Copper
Sn3.5Ag4Ti(Ce
Ga)

ABSTRACT

An Sn3.5Ag4Ti(Ce, Ga) active solder is used for joining $ZnS–SiO_2$ ceramic sputtering targets with copper backing plates at 250 °C in air. Direct soldering using the Sn3.5Ag4Ti(Ce, Ga) metal filler has been found to be a reliable and simple technique for $ZnS–SiO_2$ ceramic bonding with $ZnS–SiO_2$ and copper. The shear strengths for $ZnS–SiO_2/ZnS–SiO_2$ and $ZnS–SiO_2/Cu$ joints are 6.5 and 5.2 MPa, respectively. The bonding mechanism is described, with emphasis placed on the action of a rare earth element (Ce) and the active metal reaction. The interfacial reaction between Sn3.5Ag4Ti(Ce, Ga) filler metal and copper at temperatures ranging from 120 to 200 °C is conducted and discussed.

1. Introduction

In the conventional joining of ceramics, nickel-plated ceramics are brazed after they are metallized with the molybdenum–manganese method (Pulfrich, 1939; Nolte, 1954; Chick and Speck, 1955). Recently, direct active brazing has been developed to join ceramics to metal or to other ceramics (Elssner and Petzow, 1990; Mizuhara and Mally, 1985). The direct brazing process, without the need for premetallizing, is simpler than the molybdenum–manganese method. However, the active filler metals for ceramic brazing have a high melting point or a high conducting temperature (Chang et al., 2003a; Chai et al., 1998). For some applications, the brazing temperature is so high that it causes hot cracking or functional degradation of the ceramics. Brittle and temperature-sensitive ceramic sputtering targets are examples. In this study, an active soldering technique which provides for bonding of a ceramic target to a metal backing plate is developed. An Sn3.5Ag4Ti(Ce, Ga) filler metal was used to bond a $ZnS–SiO_2$ sputtering target with copper backing plate at 250 °C in air. Due to the low melting point of the active filler metal, the removal as well as re-bonding of the metal backing plate and ceramic sputtering target can be accomplished easily at low temperature. The effects of aging on the shear strength and interfacial microstructure are presented and discussed.

2. Experimental

The $ZnS–SiO_2$ target material used for joining in this study, supplied by Thintech Material Technology Co., Ltd., Taiwan, was a mixture of 80 at% ZnS and 20 at% SiO_2. The backing plate used for joining was commercial pure copper. The active solder Sn3.5Ag4Ti (Ce, Ga) used in this study was in the form of a

* Corresponding author.
E-mail address: changsy@yuntech.edu.tw (S.Y. Chang).
0924-0136/$ – see front matter
doi:10.1016/j.jmatprotec.2007.08.045

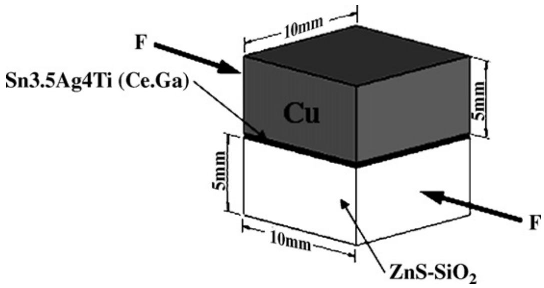

Fig. 1 – Schematic representation of the soldered specimens ready for shear testing in this study.

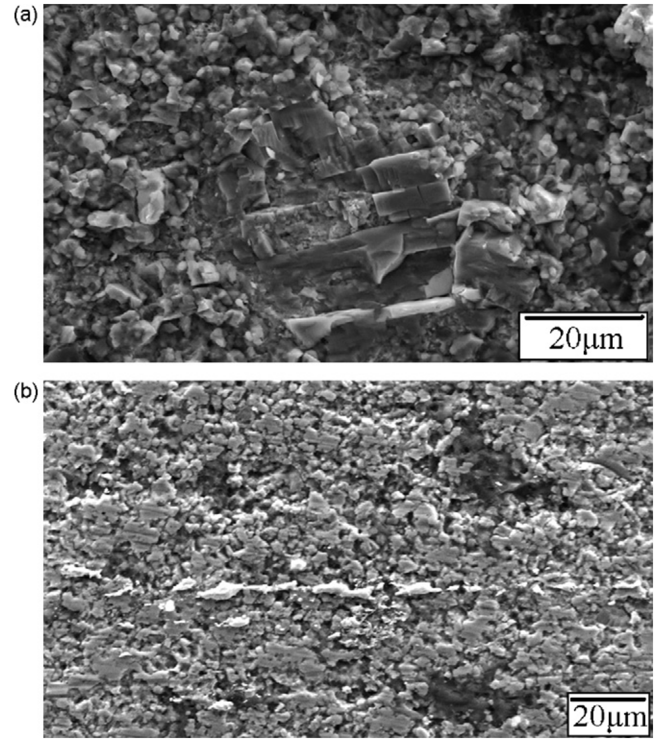

Fig. 3 – Fractographs of $ZnS–SiO_2$/Cu joint with Sn3.5Ag4Ti(Ce, Ga) active solder after tensile testing: (a) the copper specimen side; (b) the $ZnS–SiO_2$ specimen side.

0.3 mm thick plate (supplied by Euromat Co., Heinsberg, Germany). The chemical composition (wt%) of the active solder was Sn: 92.12, Ag: 3.55, Ti: 4.07, Ce: 0.12, Ga: 0.14, as analyzed. The melting range (liquidus and solidus) of this solder was between 218 and 229 °C, as analyzed by a differential scanning calorimeter at a heating rate of 10 K/min under an argon atmosphere (Chang et al., 2003b). The geometry and dimensions of the $ZnS–SiO_2$ and copper bond specimens subjected to shear testing are shown in Fig. 1.

The bonding surfaces were ground with SiC paper down to grade 1200. The soldering process was performed on an electric heat plate with thermostatic control. Prior to soldering, the $ZnS–SiO_2$ and copper were preheated on the heat plate at 250 °C. The temperature of the bond surfaces was measured by a *K*-type thermocouple. By adjusting the temperature of the heat plate until the temperature of specimens was maintained steadily. The active filler Sn3.5Ag4Ti (Ce, Ga) was then placed on the bond surfaces of $ZnS–SiO_2$ and copper. After the molten solder was agitated for 30 s, with the result that the solder was wetting on the bond surfaces, the copper specimen was placed on the $ZnS–SiO_2$. In order to conduct an interfacial reaction soundly, the $ZnS–SiO_2$ and copper specimen were rubbed together for about 30 s. After sliding and repositioning, the joints were held firmly in place and cooled down, leading to the solidification of the molten solder. The bonding strengths were measured by shear testing, as shown in Fig. 1. In order to investigate the related interfacial reactions, a set of bonded specimens was aged in a furnace from 120 to 200 °C. Cross-sectioned specimens were analyzed by an electron probe microanalyzer (EPMA) to determine the microstructures and distributions of the elements. Fractured surfaces were characterized by a scanning electron microscopy (SEM) coupled to an energy dispersion X-ray (EDX).

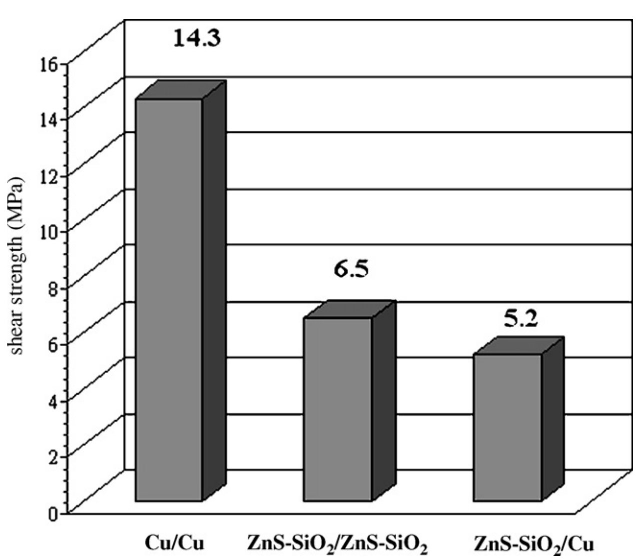

Fig. 2 – Shear strengths of Cu/Cu, $ZnS–SiO_2/ZnS–SiO_2$ and $ZnS–SiO_2$/Cu joints bonded with Sn3.5Ag4Ti(Ce, Ga) active solder.

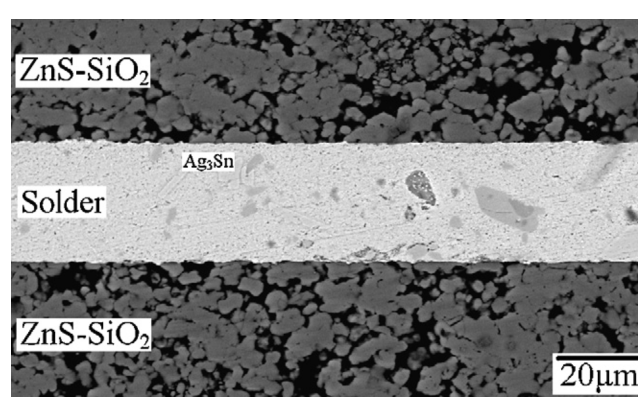

Fig. 4 – Micrograph of the $ZnS–SiO_2/ZnS–SiO_2$ joint bonded with Sn3.5Ag4Ti(Ce, Ga) active solder.

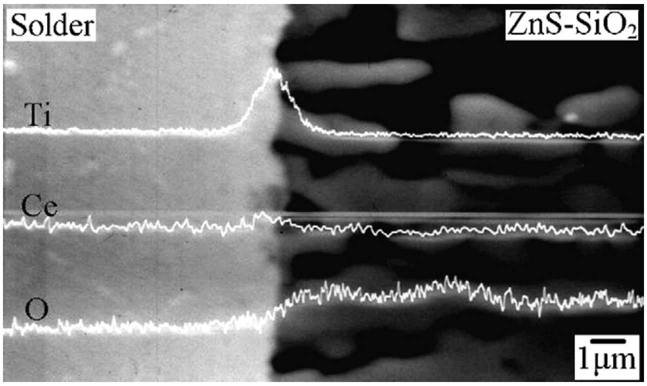

Fig. 5 – EPMA line scanning of elements across the $ZnS–SiO_2$/solder interface.

3. Results and discussion

The bonding strength of Cu/Cu, $ZnS–SiO_2/ZnS–SiO_2$, and $ZnS–SiO_2$/Cu joints using the Sn3.5Ag4Ti(Ce, Ga) solder after shear testing are given in Fig. 2. The $ZnS–SiO_2$/Cu and $ZnS–SiO_2/ZnS–SiO_2$ joints possess shear strengths of 5.2 and 6.5 MPa, respectively, which are considerably lower than that for the case of a Cu/Cu joint of similar metal. Fig. 3(a) exhibits that the fractured surface of the Cu specimen with the $ZnS–SiO_2$/Cu joint is covered with a $ZnS–SiO_2$ layer, while Fig. 3(b) provides a contrasting example of the fractured $ZnS–SiO_2$ specimen. It indicates that the $ZnS–SiO_2$/Cu joint has fractured in the $ZnS–SiO_2$ matrix.

The microstructure of the bonding interfaces of the $ZnS–SiO_2/ZnS–SiO_2$ joint using Sn3.5Ag4Ti(Ce, Ga) filler metal is shown in Fig. 4. This figure demonstrates a satisfactory joint using the active solder to bond $ZnS–SiO_2$ with $ZnS–SiO_2$. The microstructure of the Sn3.5Ag4Ti(Ce, Ga) filler metal consists of Ti-rich coarse clusters and Ag_3Sn particles. The Ti-rich clusters contain α-Ti_6Sn_5 phase (black) and the surrounding Ti_2Sn_3 phase (gray). The absence of any observable reaction phase of the interface between $ZnS–SiO_2$ and solder can be identified using a SEM and an energy dispersive spectrometer (EDX). However, EPMA elemental line scanning across the $ZnS–SiO_2$/solder interface indicates that Ti segregates at the

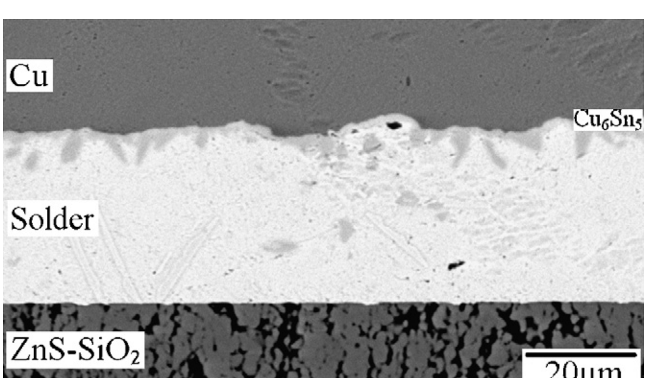

Fig. 6 – Micrograph of the $ZnS–SiO_2$/Cu joint bonded with Sn3.5Ag4Ti(Ce, Ga) active solder.

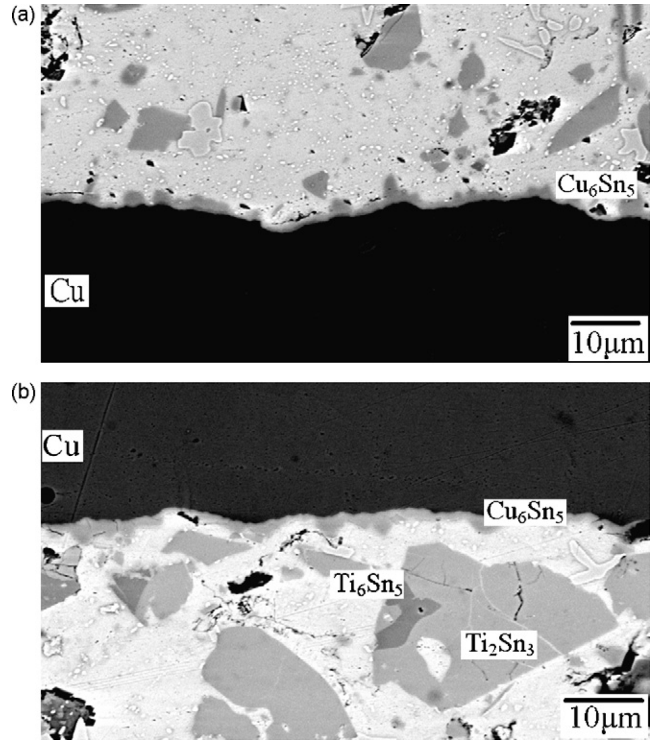

Fig. 7 – Micrograph of the solder/Cu interface of the $ZnS–SiO_2$/Cu joints bonded with Sn3.5Ag4Ti(Ce, Ga) active solder after aging test at 120 °C for 72 h (a) and 100 h (b).

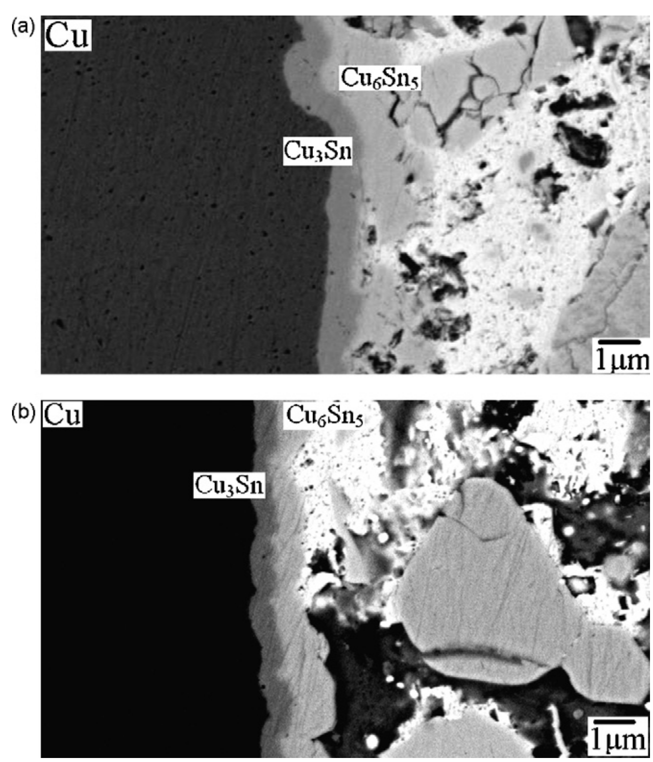

Fig. 8 – Micrograph of the solder/Cu interface of the $ZnS–SiO_2$/Cu joints bonded with Sn3.5Ag4Ti(Ce, Ga) active solder after aging test at 150 °C for 25 h (a) and 50 h (b).

interface, as shown in Fig. 5. Prior studies (Chang et al., 2003b; Chang et al., 2006) have indicated that rare earth element additions in solders promote the wetting of the active solders on ceramics and cause the reaction of the active element Ti with ceramics. The microstructure of the bounding interfaces of the $ZnS–SiO_2$/Cu joint is shown in Fig. 6. It is observed that the copper dissolves irregularly to form a scallop-shaped intermetallic compound of η-Cu_6Sn_5 phase at the solder/copper interface.

Fig. 7(a and b) show the images of the solder/Cu interfaces of $ZnS–SiO_2$/Cu joints after thermal aging at 120 °C for 72 and 100 h, respectively. They indicate that the scallop-shaped interfacial intermetallic compounds of Cu_6Sn_5 grew very slowly. After thermal aging at 150 °C, a double layer of Cu_3Sn and Cu_6Sn_5 intermetallic compounds was formed at the solder/Cu interface. Fig. 8(a and b) illustrated the solder/Cu interfaces of $ZnS–SiO_2$/solder joints after thermal aging at 150 °C for 25 and 50 h, respectively. As the aging temperature and time increased, the intermetallic compound layers became smooth. The combined ($Cu_6Sn_5 + Cu_3Sn$) intermetallic compound thickness was only about 2 μm after thermal aging at 150 °C for 75 h. Aging tests of $ZnS–SiO_2$/Cu joints caused the formation of quantities of intermetallic compounds and reduced the bonding strengths. The average shear strengths of two $ZnS–SiO_2$/solder joints after aging testing at 150 °C for 50 and 75 h are 4.37 and 3.27 MPa, respectively. A small amount of rare earth element added to solders reduces the driving force for Cu–Sn intermetallic compound formation on Cu substrates and results in inhibition of the intermetallic layer growth (Wu et al., 2004). Hence, as compared to the interface reaction of Cu with Sn-3.5Ag solder (Madeni et al., 2003), the thickness of the intermetallic compounds of the interface reaction of Cu with Sn3.5Ag4Ti(Ce, Ga) solder is much smaller. After thermal aging at 200 °C for 24 h, a double layer of Cu_3Sn and Cu_6Sn_5 intermetallic compounds was formed at the solder/Cu interface, as shown in Fig. 9(a). EPMA elemental mapping, shown in Fig. 9(b and c), indicates the segregation enrichment of Ti and Ce at the $ZnS–SiO_2$/solder interface, which was also observed in prior studies of ITO/Cu and alumina/Cu joints with the active solder Sn3.5Ag4Ti(Ce, Ga) (Chang et al., 2003b; Chang et al., 2007).

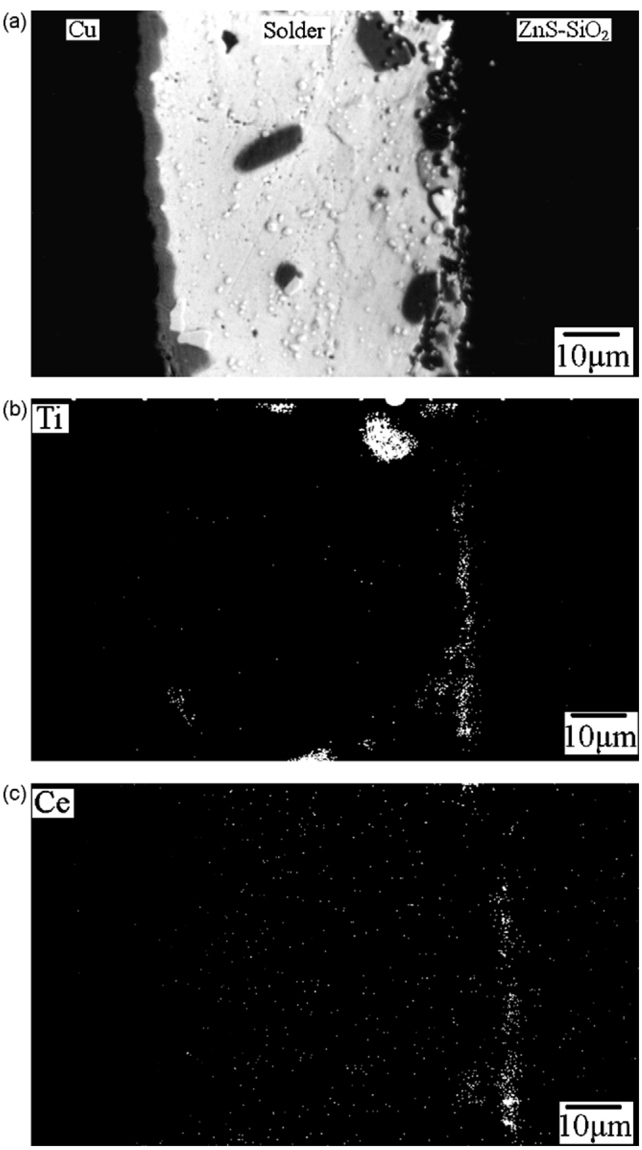

Fig. 9 – Micrograph and EPMA analyses of the $ZnS–SiO_2$/Cu joint bonded with Sn3.5Ag4Ti(Ce, Ga) active solder after aging test at 200 °C for 24 h: (a) the interfacial microstructure; (b) elemental mapping of Ti; (c) elemental mapping of Ce.

4. Conclusion

In this study, a fluxless low temperature bonding technique is developed to join $ZnS–SiO_2/ZnS–SiO_2$ and $ZnS–SiO_2$/Cu in air using an active solder, Sn3.5Ag4Ti(Ce, Ga). The bond shear strengths of Cu/Cu, $ZnS–SiO_2/ZnS–SiO_2$, and $ZnS–SiO_2$/Cu joints are determined to be 14.3, 6.5, and 5.2 MPa, respectively. Fractography of the shear-tested specimens show that the $ZnS–SiO_2$/Cu joint failure occurred in the $ZnS–SiO_2$ matrix. The rare earth element (Ce) additions in solder promote the wetting of the active solder on $ZnS–SiO_2$ and cause the reaction of Ti with $ZnS–SiO_2$ at bonding temperature (250 °C). EPMA elemental mapping revealed a tendency of Ti to segregate at the $ZnS–SiO_2$/solder interfaces. During $ZnS–SiO_2$/Cu soldering, copper is found to dissolve into Sn3.5Ag4Ti(Ce, Ga) solder to form scallop-shaped Cu_6Sn_5 intermetallic compounds. A small amount of a rare earth element in solder can inhibit the intermetallic layer growth. After thermal aging at 150 °C for 75 h, the thickness of the intermetallic compounds is only about 2 μm. Nevertheless, aging tests enhanced the segregation of Ti and Ce at the $ZnS–SiO_2$/solder interfaces. Aging tests of $ZnS–SiO_2$/Cu joints caused the formation of quantities of Cu–Sn intermetallic compounds and reduced the bonding strengths.

Acknowledgments

Special thanks go to National Science Council, Taiwan, for sponsoring this research under Grant No. NSC-95-2221-E-002-160.

REFERENCES

Chang, S.Y., Hung, Y.T., Chuang, T.H., 2003a. Joining alumina to Inconel 600 and UMCo-50 superalloys using an Sn10Ag4Ti active filler metal. J. Mater. Eng. Perform. 12, 123–127.

Chai, Y.H., Weng, W.P., Chuang, T.H., 1998. Relationship between wettability and interfacial reaction for Sn10Ag4Ti on Al_2O_3 and SiC substrates. Ceram. Int. 24, 273–279.

Chang, S.Y., Tsao, L.C., Chiang, M.J., Chuang, T.H., 2003b. Active soldering of indium tin oxide (ITO) with Cu in air using an Sn3.5Ag4Ti(Ce, Ga) filler. J. Mater. Eng. Perform. 12,383–389.

Chang, S.Y., Lu, M.H., Tsao, L.C., Chuang, T.H., 2006. Active soldering of ITO to copper: active soldering of indium-tin-oxide (ITO) sputtering targets to Cu backing plates using an Sn56Bi4Ti(Ce, Ga) filler. Weld. J. 4, 81–83.

Chang, S.Y., Chuang, T.H., Yang, C.L., 2007. Low temperature bonding of alumina/alumina and alumina/copper in air using an Sn3.5Ag4Ti(Ce. Ga) filler. J. Electron. Mater. 36 (9), 1193–1198.

Chick, A.J., Speck, L.J., 1955. Fabrication of metal to ceramic seals, U.S. Patent 2,708,787.

Elssner, G., Petzow, G., 1990. Metal/ceramic joining. ISIJ Int. 30, 1011–1032.

Mizuhara, H., Mally, K., 1985. Ceramic-to-metal joining with active brazing filler metal. Weld. J. 10, 27–32.

Madeni, J., Liu, S., Siewert, T., 2003. Intermetallics formation and growth at the interface of tin-based solder alloys and copper substrates. In: 2nd International Brazing and Soldering Conference (ISBC), 17–19 February, San Diego, California, USA.

Nolte, H.J., 1954. Metalized ceramic, U.S. Patent 2,667,432.

Pulfrich, H., 1939. Ceramic-to-metal seal, U.S. Patent 2, 163,407.

Wu, C.M.L., Yu, D.Q., Law, C.M.T., Wang, L., 2004. Properties of lead-free solder alloys with rare earth element additions. Mater. Sci. Eng. R44, 1–44.